

Flexural Property of String Beam of Pre-Stressed Glulam Based on Influence of Regulation and Control

Nan Guo^{1,*}, Wenbo Wang¹ and Hongliang Zuo¹

Abstract: Applying pre-stress in glulam beam can reduce its deformation and make full use of the compressive strength of wood. However, when the glulam with low strength and the pre-stressed steel with high strength form combined members, materials of high strength can't be fully utilized. Therefore, this study puts forward the idea of regulating and controlling string beam of pre-stressed glulam. By regulating and controlling the pre-stress, a part of the load borne by the wood is allocated to the pre-stressed tendon, which is equivalent to completing a redistribution of internal force, thus realizing the repeated utilization of the wood strength and the full utilization of the strength of the high-strength pre-stressed tendon. The bending experiments of 10 beams under 5 working conditions are carried out. The failure mode, bearing capacity and deformation of the beams are analyzed. The results show that 90% of beams are deformed under compression. The ultimate load of the regulated and controlled beam is obviously larger than that of the unregulated beam, and the ultimate load of the beam increases with the increase of the degree of regulation and control. Compared with that of the unregulated beams, the ultimate load of beams regulated by 7.5%-30% increases by 25.42%-65.08%, and the regulated and controlled effect is obvious. With the increase of the regulation and control amplitude of pre-stress, the stiffness of string beam of pre-stressed glulam increases. In addition, with the increase of the regulation and control amplitude, the compression height of the beam increases before the failure, and it reaches the state of full-section compression at the time of failure, giving full play to the compressive property of the glulam. At the end of the experiment, the constitutive relation which can reflect the anisotropy of the wood is established combined with the experimental data. The finite element analysis of the beam under 7 working conditions is carried out by using ABAQUS finite element program, and the influence of the regulation and control amplitude on the stress distribution and ultimate bearing capacity of the beam is discussed.

Keywords: String beam of glulam, flexural property, experimental study, pre-stress, regulation and control.

1 Introduction

The wood products in different shapes and sizes glued by several boards with thickness of more than 18 mm and less than 45 mm, and moisture content of less than 18% are

¹ School of Civil Engineering, Northeast Forestry University, Harbin, 150040, China.

* Corresponding Author: Nan Guo. Email: snowguonan@163.com.

called laminated glulam, simply called glulam. Compared with logs, glulam has many advantages such as small variability, high reliability, full use of wood strength, and the size of components is not limited by the natural size [Guo, Chen and Zhang (2016); Toratti, Schnabl and Turk (2014); Green, Winandy and Kretschmann (1999)]. However, there are some problems in the glulam beams. For example, in the glulam beams, the compressive strength of wood cannot be fully utilized; brittle failure of glulam beams often occurs under bending; the deformation of glulam beams is large, and the section size is often controlled by the deformation. In view of the shortcomings of traditional glulam beams, the project group put forward a new string beam of pre-stressed glulam in the early stage. When the beam is subjected to load, the upper glulam bears compressive stress, the lower pre-stressed steel wire bears tensile stress, and the bending moment caused by external load is balanced by the tensile pressure pair of the two. Applying pre-stress in glulam can make full use of reinforcing steel and glulam, can reduce the deformation of glulam beam, can reduce or eliminate the increase of deformation caused by the creep deformation of wood by adjusting the size of pre-stress [Guo, Jiang and Zuo (2017); Yahyaei-Moayyed and Taheri (2011a); Yahyaei-Moayyed and Taheri (2011b)], as well as can effectively improve the strength of compression zone of glulam section to make full use of the compressive strength of wood and save materials. In addition, if pre-stress is applied, the glulam beam can be broken under compression rift grain. When wood's rift grain is under compression, the fiber will blend under compression, and the surface of the experiment specimen will be wrinkled and show obvious plastic deformation.

As can be seen from the above, it has many advantages to apply pre-stress in the glulam. However, when the glulam with low strength and the pre-stressed steel with high strength form a combined member, the high-strength material is often not fully utilized. The application of pre-stress can improve the above situation to a certain extent, but the tensile stress on the top of the glulam should be controlled to be less than the tensile strength before the external load in the application stage of pre-stress, which limits the use of pre-stress. The experimental results of the project group show that the stress in the steel wire can only reach about 280 Mpa in order to ensure that the glulam on the top of beam is not damaged in the application of pre-stress. When the beam is broken, the stress of the steel wire is about 800 Mpa. However, the design value of the tensile strength of the steel wire is 1100 Mpa, so the strength of the steel wire has not been fully utilized. Therefore, this study puts forward the concept of regulation and control of pre-stress which is realized by the horizontal tension device for screw thread tension put forward by the project group. Every time the pre-stress is adjusted, it means that a part of the load borne by the wood is allocated to the pre-stressed tendon, which is equivalent to completing a redistribution of the internal force, thus realizing the repeated utilization of the wood strength and the full utilization of the strength of the high-strength pre-stressed tendon.

At present, scholars at home and abroad have carried out a series of researches on the mechanical properties of glulam beams [Fava, Carvelli and Poggi (2013); Franke, Franke and Harte (2015); Sinha, Way and Mlasko (2014); Issa and Kmeid (2005)] in order to strengthen glulam with new materials [Uzel, Togay, Anil et al. (2017); Ribeiro, Abílio, Lima et al. (2009); Ferrier, Labossière and Neale (2012); Yang, Liu, Lu et al. (2016); Wei, Ji, Duan et al. (2017); Anshari, Guan, Kitamori et al. (2012); Zhong, Wu, Ren et al. (2017); Fang, Sun, Liu et al. (2015)]. In order to improve the flexural property of glulam

beams, make full use of materials and increase the application scope of glulam beams, scholars at home and abroad put forward the idea of applying pre-stress to ordinary wood beams and glulam beams, and made a series of explorations, mainly including two aspects: application of pre-stress through stretching the pre-stressed tendon and tensioning fibre materials [Guo, Wang and Zuo (2017); Luca and Marano (2012); D'Aveni and D'Agata (2017); McConnell, McPolin and Taylor (2014); Yang, Ju, Liu et al. (2016); Guan, Rodd and Pope (2005); Negrão (2016)]. At present, scholars at home and abroad haven't carried out the research on the flexural property of string beams of pre-stressed glulam based on the influence of regulation and control, so this study is of great significance.

To study the failure form, bearing capacity and deformation of beams with different degree of regulation and control, and to define the influence of pre-stress regulation and control on the flexural property of beams, this study conducts loading failure experiment of glulam beam by applying pre-stress to the glulam beams, adding external load and adjusting the deflection of beams to the degree when the external load is not added. Combined with the experimental data, the elastic-plastic constitutive relation suitable for the anisotropy of glulam is obtained and analyzed by ABAQUS finite element program [Guo, He and Chen (2015)]. By changing the regulation and control amplitude of pre-stress in a wider range, the influence of the regulation and control amplitude on the stress distribution and ultimate bearing capacity of beam section is discussed. According to the principle that the material stress is not greater than its strength in the stage of applying pre-stress and load, the boundary of pre-stress regulation and control is found, and the reasonable regulation and control range of pre-stress is obtained.

2 Introduction of experiment

2.1 Experimental flow

In order to study the failure form, bearing capacity and deformation of string beams of glulam under different degree of pre-stress regulation and control and define the influence of pre-stress regulation and control on its flexural property, this study conducts and experiment and the experimental flow is as follows. First, pre-stress is applied to the beam to obtain its inverse arch value. Then the initial loads of different degrees are applied to make the beam produce a certain deflection. Next, the deflection of the beam is adjusted to the degree before the initial load is added by the pre-stress regulating device. Finally, the beam loading experiment is carried out according to the loading mechanism until the beam is destroyed. The deformation of beam from the initial loading to the end of regulation and control is shown in Fig. 1.

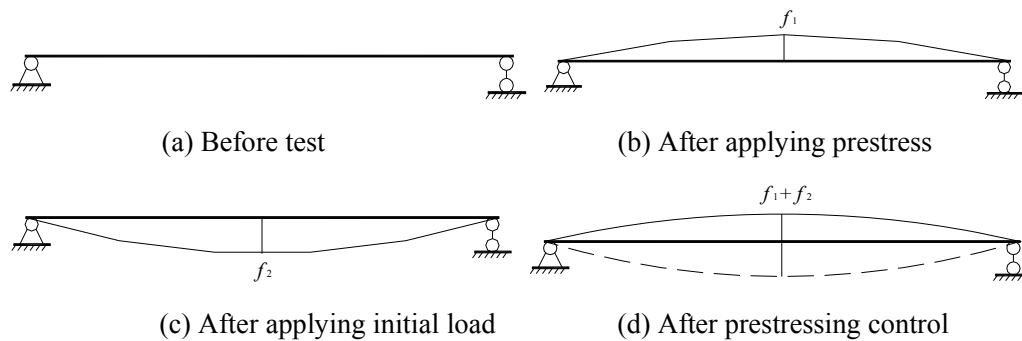


Figure 1: Deformation of beam in the process of loading

2.2 Grouping of experiment

According to the purpose of the experiment, 10 string beams of glulam with geometric scale of 1:2 are made, and the reasonable number of steel wires and pre-stressed value obtained by the project group are adopted, namely, 4 steel wires for each beam, 9 kN for each beam, which is in Group A. 5 working conditions are divided according to the regulation and control amplitude of pre-stress and each working condition includes 2 identical beams, including 2 beams that are not regulated and beams with the regulation amplitude of 7.5%, 15%, 22.5% and 30% respectively. The detailed grouping of string beams of glulam for the experiment in Tab. 1. The ultimate load of the beam in the table is obtained from the previous experiment of the project group.

Table 1: Grouping of beams for experiment

Beam number	Size/mm	Number of beams	Prestressing value/kN	Degree of regulation
YA1	3150×80×100	2	9	-
YTA2	3150×80×100	2	9	7.5% of ultimate load
YTA3	3150×80×100	2	9	15% of ultimate load
YTA4	3150×80×100	2	9	22.5% of ultimate load
YTA5	3150×80×100	2	9	30% of ultimate load

Note: In the beam number YTAx in the table, Y represents the application of pre-stress, T represents pre-stress regulation and control, A represents the string beam group of glulam under bending test, and x represents the serial number of working condition.

3 Experiment result and analysis

3.1 Ultimate load and failure mode

At the end of the experiment, the ultimate load and failure mode of beams under each condition are summarized in Tab. 2.

Table 2: Ultimate load and failure mode of beams

Groups	Beam number	Ultimate load/kN		Failure mode
		experimental value	Average value	
Unregulation	YA1-1	32.33	33.36	Failure of beam roof under compression
	YA1-2	34.38		Failure of beam bottom under tension
Regulation 7.5%	YTA2-1	39.05	41.84	Failure of beam roof under compression
	YTA2-2	44.64		Failure of beam roof under compression
Regulation 15%	YTA3-1	49.50	50.34	Failure of beam roof under compression
	YTA3-2	51.19		Failure of beam roof under compression
Regulation 22.5%	YTA4-1	56.34	53.17	Failure of beam roof under compression
	YTA4-2	49.99		Failure of beam roof under compression
Regulation 30%	YTA5-1	56.31	55.07	Failure of beam roof under compression
	YTA5-2	53.83		Failure of beam roof under compression

It can be seen from Tab. 2 that the top of beams are not damaged except the YA1-2 beam of unregulated group is damaged by compression for knag at the bottom of the beam. The damages part reaches 90% of the total damage amount. This shows that regulation and control can obviously improve the failure mode of string beam of glulam and make full use of the compressive property of wood. Tab. 2 shows that the ultimate load of the regulated beam is obviously larger than that of the unregulated beam, and the ultimate load of the beam increases with the increase of the regulation and control amplitude. Compared with the unregulated beams, the ultimate load of beams with the regulation of 7.5%-30% increases by 25.42%-65.08%, and the regulation and control effect is obvious. As the regulation and control amplitude increases, the change trend of the ultimate load is shown in Fig. 2.

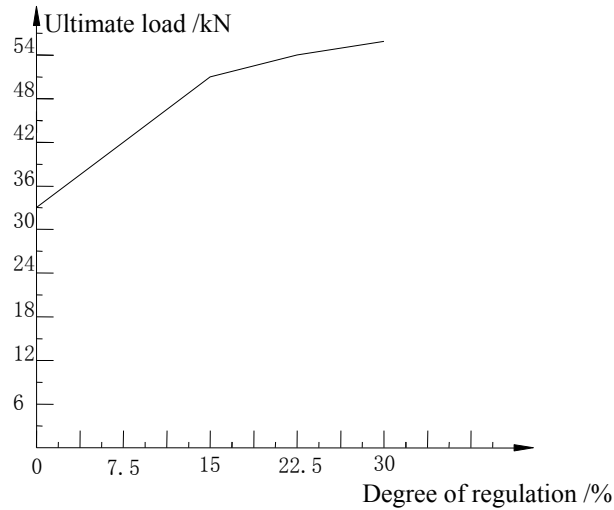


Figure 2: Change trend of the ultimate load

As can be seen from Fig. 2, when the regulation and control amplitude is 7.5% and 15%, the ultimate load increases linearly and the regulation and control effect is obvious; when the regulation and control amplitude is 22.5% and 30%, the ultimate load increases slowly, showing that regulation and control cannot increase the ultimate load greatly.

3.2 Load-deflection curve

One of the two experiment beams for each condition is selected to draw its load-deflection curve, as shown in Fig. 3.

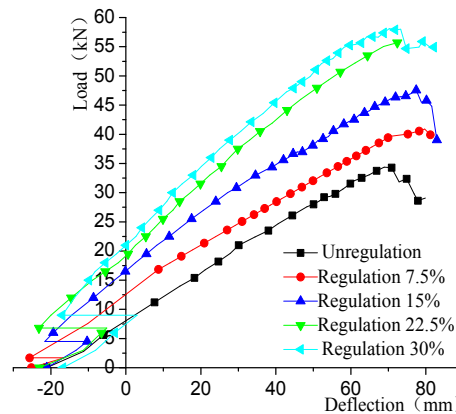


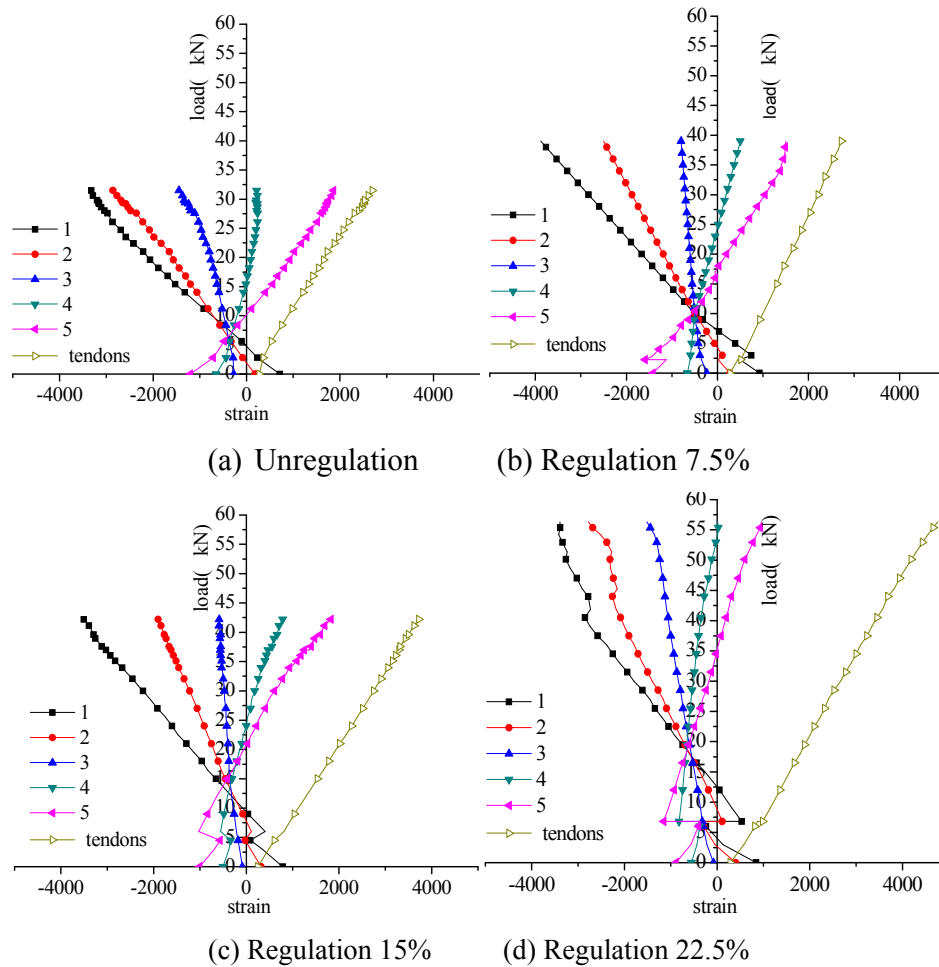
Figure 3: Load-deflection curve of each beam

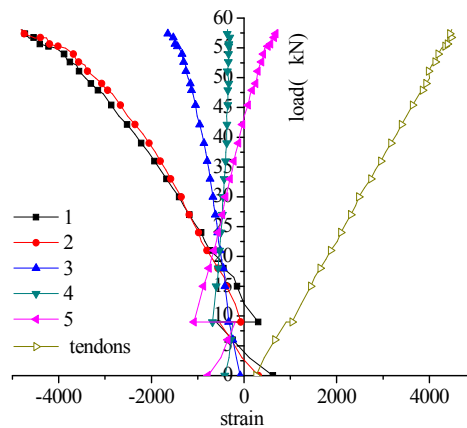
As can be seen from Fig. 3, the slope and peak value of the load-deflection curve increase as the pre-stress regulation and control amplitude increases, that is, the stiffness and the bearing capacity of the beam increase. The larger the regulation and control amplitude is,

the larger the arm of force at the string point is, which increases the stiffness and bearing capacity of the beam. In addition, regulation and control changes the stress distribution of the glulam part so that the top of the beam is under tension and the bottom of the beam is under compression, which is just opposite to the stress state at the time of failure, which is beneficial to the bearing capacity of the beam.

3.3 Load-strain curve

The load-strain curve of string beam of glulam is obtained by experiment, as shown in Fig. 4.





(e) Regulation 30%

Figure 4: Load-strain curve of each beam

The load-strain curve reflects the change of the strain distribution as the external load increases. When the strain is negative (the curve is on the left side of the Y axis), the material is under compression. When the strain is positive (the curve is on the right side of the Y axis), the material is under tension. As can be seen from Fig. 4, at the initial stage of loading, the top of beam is tensioned and the bottom of beam is compressed. At the beginning of loading, the compression strain on the top of unregulated beam and tension strain at the bottom of unregulated beam decrease gradually. When the load reaches about 5 kN, the bottom of the beam begins to be tensioned, and then the compression strain on the top of beam and tension strain at the bottom of beam increase gradually until failure. For regulated beam, at the beginning of loading, the compression strain on the top beam and tension strain at the bottom decrease gradually. There is obvious strain mutation in the regulation and control so that the previously gradually decreased strain recovers, which is equivalent to delaying the strain development process of glulam. When the load continues to be put, the strain change trend is similar to that of the unregulated beam, but the load at the bottom of beam increases to 15-45 kN, and the larger the regulation and control is, the more the load increases when the bottom of beam begins to be tensioned.

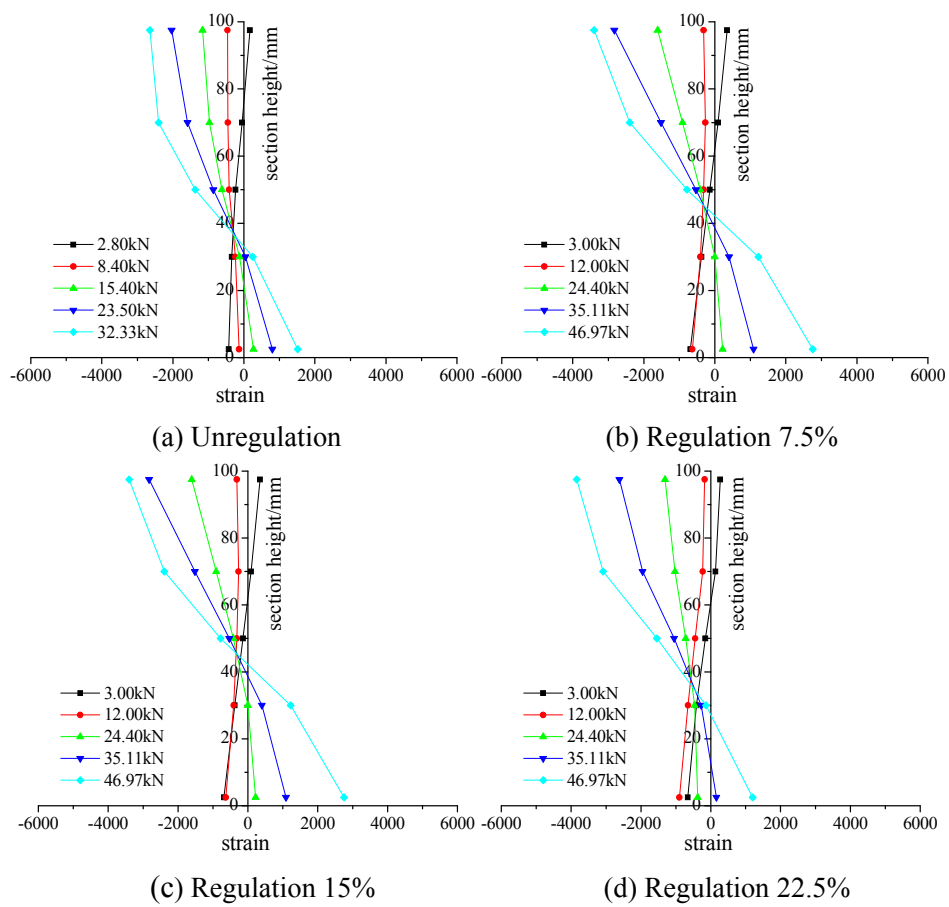
Fig. 4 shows that the tension strain at the bottom of beam is generally between 1500 and 2000 $\mu\epsilon$ at the time of failure. The tension strain is so small that it does not reach 4630 $\mu\epsilon$ corresponding to the tensile strength. However, the top compression strain of beam during failure is generally between 3500 and 4000 $\mu\epsilon$, which has reached the compression strain of 3640 $\mu\epsilon$ corresponding to the compressive strength, so it is directly crushed.

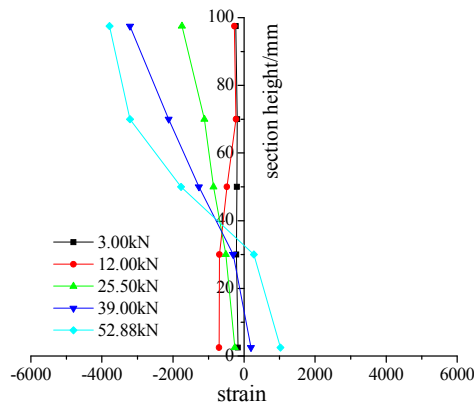
There are 3 layers of glued plates in compression zone when the beams in unregulated group and regulated groups of 7.5% and 15% are damaged and there are 4 layers of glued plates in compression zone when the beams in unregulated group and regulated groups of 22.5% and 30% are damaged. This shows that the compression height of beam increases before the failure with the increase of the regulation and control amplitude, and it reaches the state of full section compression at the time of failure, fully exerting the compressive strength of the glulam.

4 Theoretical analysis

4.1 Validation of plane cross-section assumption

In order to observe more clearly the stress and strain of the three-point section of the string beam of glulam in each stage of loading, the strain curve of the three-point position along the beam height direction under each grade of load is drawn, as shown in Fig. 5, where x-axis represent the strain of the wood, the negative represents the compression of the wood, the positive represents the tension of the wood, and y-axis represents the height of the wood section. The original point is the bottom of the wood. The point of intersection of each curve with the y-axis is the position of the central axis.





(e) Regulation 30%

Figure 5: Strain curve along the beam height

It can be seen from Fig. 5 that the strain curve of the three-point position along the beam height direction is approximately linear distribution under each grade of load. When the load is large, the strain in the compression area of the section of some beams suddenly reduces because the data measured by the strain gauge changes abruptly due to the wrinkling of the wood in the compression area or the cracking of the wood in the tension area. The number of beams with such phenomena is not large when the load is large. Therefore, it can be considered that the strain change along the beam height of string beam of glulam conforms to the plane cross-section assumption.

4.2 Derivation of bearing capacity formula

The bearing capacity formula of string beam of glulam is derived on the basis of the following assumptions: ① when the glulam beam reaches the bearing capacity ultimate state, the glulam on the top of the beam reaches the ultimate compression strain; ② conforming to the plane cross-section assumption in the range of glulam section; ③ Glulam conforms to the rift grain constitutive relation of typical wood materials, as shown in Fig. 6.

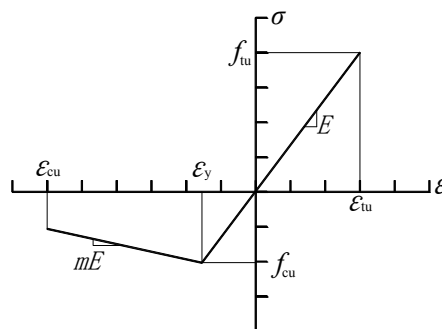


Figure 6: Rift grain constitutive relation of wood materials

As can be seen from Fig. 6, the expression for the rift grain constitutive relation of the wood materials is:

$$\sigma = \begin{cases} E\varepsilon & (-\varepsilon_y \leq \varepsilon < \varepsilon_{tu}) \\ f_{cu} + mE(\varepsilon - \varepsilon_y) & (-\varepsilon_{cu} < \varepsilon < -\varepsilon_y) \end{cases} \quad (1)$$

where,

σ -Stress of wood materials(N/mm²);

E -elasticity modulus of wood materials(N/mm²);

ε -Strain of wood materials;

ε_y -Compression strain of wood materials;

ε_{cu} -Ultimate compression strain of wood materials;

ε_{tu} -Ultimate tension strain of wood materials;

f_{cu} -Compressive strength of wood materials(N/mm²);

m -Ratio of slope to elasticity modulus of the falling section of the constitutive curve of wood materials under compression

According to the previous experimental data, when the maximum reinforcement ratio is estimated,

$\varepsilon_{cu}=1.2\%$, $\varepsilon_y=0.35\%$, $m=-0.2$ of glulam material is selected.

(1) When the bottom of glulam is cracked under tension, its bearing capacity calculation formula is derived as follows:

If the pre-stress is small, the bottom of the pre-stressed wood beam is first cracks under tension, namely $\sigma_t > f_b$, and then the steel wire bears the entire tension until the top of the glulam reaches the ultimate compression strain, the steel wire just bends, and the beam reaches the bearing capacity ultimate state. The calculation diagram is shown in Fig. 7.

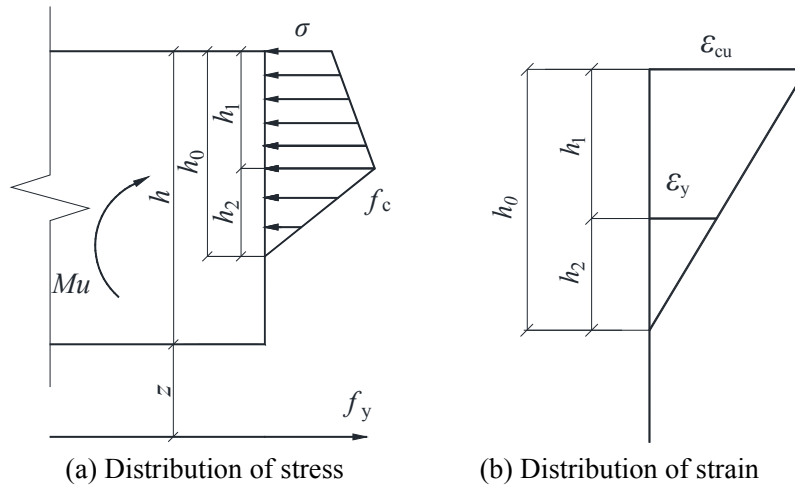


Figure 7: Calculation diagram when bottom of glulam is broken by tension

It can be obtained from force balance that:

$$\frac{1}{2}(\sigma + f_c)h_1b + \frac{1}{2}f_c h_2b = f_y A_s \quad (2)$$

The ultimate bearing capacity of the section can be obtained from the bending moment balance:

$$M_u = M_1 + M_2$$

Where,

$$M_1 = \sigma h_1 b (h + z - \frac{1}{2}h_1) + \frac{1}{2}(f_c - \sigma)h_1 b (h + z - \frac{2}{3}h_1) + \frac{1}{2}f_c h_2 b (h + z - h_1 - \frac{1}{3}h_2) \quad (3)$$

where,

Σ -The compression stress corresponding to the ultimate compression strain of the beam top of pre-stressed glulam is $\sigma = f_c + mE(\varepsilon_{cu} - \varepsilon_y)$. When there is experimental data, it can be calculated according to the value of experimental data;

h_1, h_2 -The section height (mm) of the stress of the falling section and the rising section of the compression zone of glulam can be obtained according to the strain relation of the typical wood materials by $\frac{h_2}{h_0} = \frac{\varepsilon_y}{\varepsilon_{cu}}$, where, h_0 is the total section height of compression zone of glulam. When there is experimental data, it can be calculated according to the experimental data;

z -Distance from wire to bottom of glulam beam;

M_u -Ultimate bearing capacity of pre-stressed glulam beam (kN/m);

M_1 -Bending moment value caused by the action of glulam beam and steel wire;

M_2 -Bending moment value caused by pre-tightening force of steel wire end's translation to beam centroid during pre-loading;

P -Preloading value;

e -Distance between steel wire end anchorage position and beam centroid.

(2) When the bottom of glulam is not cracked under tension, its bearing capacity calculation formula is derived as follows:

When the pre-stress is large, the bottom of glulam is not cracked under tension, namely, $0 < \sigma \leq f_t$. the glulam and the steel wire at the beam bottom jointly bear tension until the top of glulam reaches the ultimate compression strain, the steel wire just bends, and the beam reaches the bearing capacity ultimate state. The calculation diagram is shown in Fig. 8.

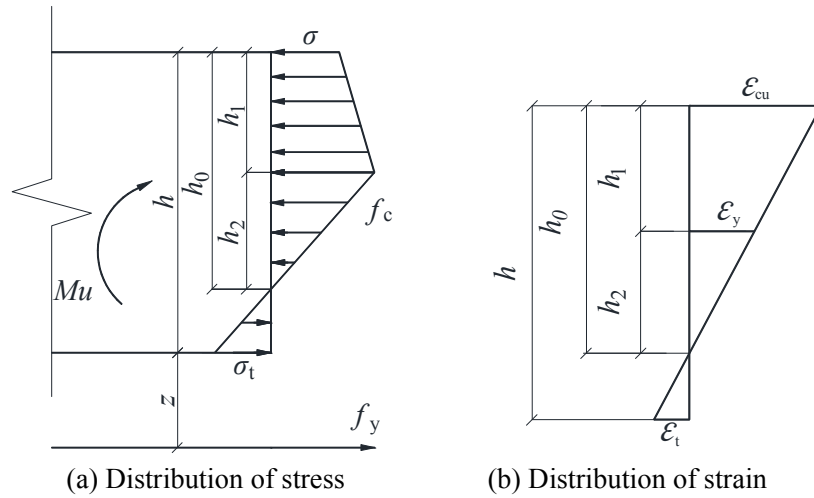


Figure 8: Calculation diagram when bottom glulam is not broken by tension

It can be obtained from force balance that:

$$\frac{1}{2}(\sigma + f_c)h_1b + \frac{1}{2}f_ch_2b = f_yA_s + \frac{1}{2}\sigma_t(h - h_1 - h_2)b \tag{4}$$

It can be obtained from bending moment balance that:

$$M_u = M_1 + M_2$$

where,

$$M_1 = \sigma h_1 b \left(h + z - \frac{1}{2}h_1 \right) + \frac{1}{2}(f_c - \sigma)h_1 b \left(h + z - \frac{2}{3}h_1 \right) + \frac{1}{2}f_ch_2b \left(h + z - h_1 - \frac{1}{3}h_2 \right) - \frac{1}{2}\sigma_t(h - h_1 - h_2)b \left(\frac{1}{3}(h - h_1 - h_2) + z \right) \tag{5}$$

$$M_2 = Pe$$

where,

σ_t -Tensile stress of glulam at the bottom of pre-stressed glulam beam, $\sigma_t = E\epsilon_t$;

ϵ_t -Tension strain of glulam at the bottom of pre-stressed glulam beam can be obtained

according to the strain relation shown in Fig. 8 by $\frac{h - h_0}{h_0} = \frac{\epsilon_t}{\epsilon_{cu}}$.

The bottom of the glulam beam is $\sigma_t = 0$, the steel wire bears the full tension until the top of the glulam reaches the ultimate compression strain, the steel wire just bends, and the beam reaches the ultimate state of the bearing capacity, and the calculation diagram is shown in Fig. 9.

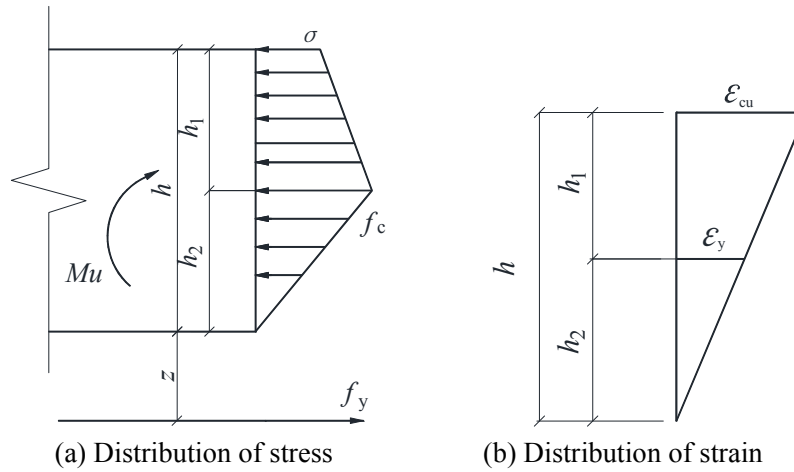


Figure 9: Calculation diagram

It can be obtained from force balance that:

$$\frac{1}{2}(\sigma + f_c)h_1b + \frac{1}{2}f_ch_2b = f_yA_s \quad (6)$$

The ultimate bearing capacity of section obtained from bending moment balance is:

$$M_u = M_1 + M_2$$

where,

$$M_1 = \sigma h_1 b \left(h + z - \frac{1}{2}h_1 \right) + \frac{1}{2}(f_c - \sigma)h_1 b \left(h + z - \frac{2}{3}h_1 \right) + \frac{1}{2}f_ch_2b \left(h + z - h_1 - \frac{1}{3}h_2 \right) \quad (7)$$

5 Finite element analysis

In order to change the regulation and control amplitude of pre-stress in a wider range, the influence of the regulation and control amplitude on the stress distribution and ultimate bearing capacity of beam section is discussed. According to the principle that the material stress is not greater than its strength in the pre-stressing and loading stage, the boundary of pre-stress regulation and control is found, and the reasonable regulation and control range of pre-stress is given. After the bending experiment, the constitutive relation of anisotropy of wood has been established combined with the experimental data, and the finite element analysis is carried out by using ABAQUS finite element program.

5.1 Modeling process

(1) Component creation and assembly

According to the experiment conditions and the actual loading features of string beam of pre-stressed glulam, the finite element analysis model is simplified reasonably. As shown in Fig. 10, the components of the finite element model include: glulam beam, steel wire, end base plate, deviator, screw rod, steel base plate and support. After each component has been created, the components are assembled according to the actual position in the experiment beam. The string beam of pre-stressed glulam after assembly is shown in Fig. 11.

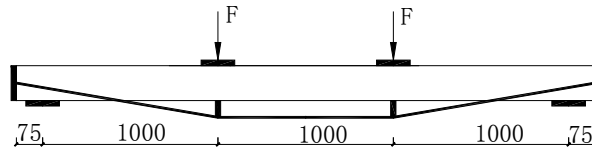


Figure 10: Simplified model



Figure 11: String beam of pre-stressed glulam after assembly

(2) Constitutive relation

The finite element model established in this study includes glulam and steel materials, of which steel materials are subdivided into high-strength pre-stressed steel wire and Q345 steel plate. Therefore, it is necessary to define three kinds of material properties.

Wood is a kind of non-homogeneous anisotropic natural material, which is complicated in itself and cannot directly apply the constitutive model commonly used in ABAQUS finite element analysis software. In view of the anisotropic characteristics of wood and the nonlinear characteristics of glulam in the course of stress, the anisotropic elastic-plastic constitutive relation is adopted for analysis. The specific setting is as follows: when defining elastic properties of glulam beam, the type is selected as orthogonal anisotropy. The stiffness matrix of anisotropic materials in ABAQUS is:

$$\begin{bmatrix} D_{1111} & D_{1122} & D_{1133} & 0 & 0 & 0 \\ & D_{2222} & D_{2233} & 0 & 0 & 0 \\ & & D_{3333} & 0 & 0 & 0 \\ & & & D_{1212} & 0 & 0 \\ & & & & D_{1313} & 0 \\ & & & & & D_{2323} \end{bmatrix}$$

where,

$$D_{1111} = E_1(1 - \nu_{23}\nu_{32})r,$$

$$D_{2222} = E_2(1 - \nu_{13}\nu_{31})r,$$

$$D_{3333} = E_3(1 - \nu_{12}\nu_{21})r,$$

$$D_{1122} = E_1(\nu_{21} + \nu_{31}\nu_{23})r = E_2(\nu_{12} + \nu_{32}\nu_{13})r,$$

$$\begin{aligned}
 D_{1133} &= E_1(v_{31} + v_{21}v_{32})r = E_3(v_{13} + v_{12}v_{23})r, \\
 D_{2233} &= E_2(v_{32} + v_{12}v_{31})r = E_3(v_{23} + v_{21}v_{13})r, \\
 D_{1212} &= G_{12}, \\
 D_{1313} &= G_{13}, \\
 D_{2323} &= G_{23}.
 \end{aligned}$$

$$r = \frac{1}{1 - v_{12}v_{21} - v_{23}v_{32} - v_{31}v_{13} - 2v_{21}v_{32}v_{13}}$$

For wood, the three basic axes used for mechanical analysis are longitudinal axis, radial axis and chord axis. The basic axes of wood are shown in Fig. 12. For glulam materials, the radial and chord axes of wood are generally not distinguished due to their manufacturing characteristics. Instead, both are collectively referred to as the horizontal axis of glulam [Zhao (2015)]. In this study, the direction of glulam fiber is “1”, and the radial and chord directions are “2” and “3” respectively. There are $D_{2222}=D_{3333}$, $D_{1313}=D_{1212}$, $D_{1133}=D_{1122}$. The stress-strain curve (constitutive curve) is drawn according to compression experimental result of typical glulam prismoid, as shown in Fig. 13. According to the document [Green, Winandy and Kretschmann (1999)], the elasticity modulus, shear modulus and Poisson’s ratio of glulam are obtained. And then the parameters in the stiffness matrix of glulam required in ABAQUS are calculated, as shown in Tab. 3. In defining the plastic property of the glulam beam, the yield stress is 35 N/mm².

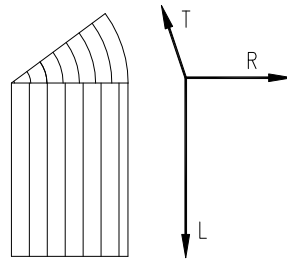


Figure 12: Basic axes of wood

Table 3: Parameters in the stiffness matrix of glulam

D_{1111}	D_{2222}	D_{3333}	D_{1212}	D_{1313}	D_{1122}	D_{1133}	D_{2323}	D_{2233}
8654.08	488.53	488.53	564.57	564.57	221.98	221.98	150.55	182.10

Note: The unit in the table is N/mm².

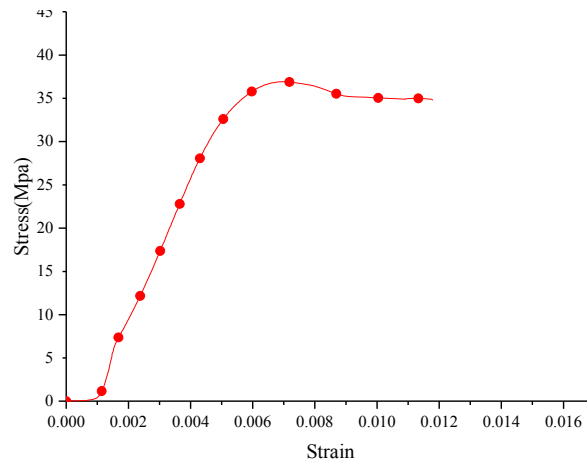


Figure 13: Stress-strain curve of prismoid

(3) Analysis of initial setting and loading

According to the experiment, the model is set to 5 analysis steps, including: initial analysis step, application of pre-stress, application of initial load, regulation and control of pre-stress, application of failure load. The application of pre-stress and the regulation and control process of pre-stress are realized by adjusting the length of the screw rod. In the corresponding analysis step, the load is created, the load category is defined as mechanics, the analysis type is bolt load, and the regulation length of the screw rod is determined according to the required pre-stress value and regulation value. The process of applying failure load by the jack is achieved by applying concentrated load. The simulated loading diagram is shown in Fig. 14.

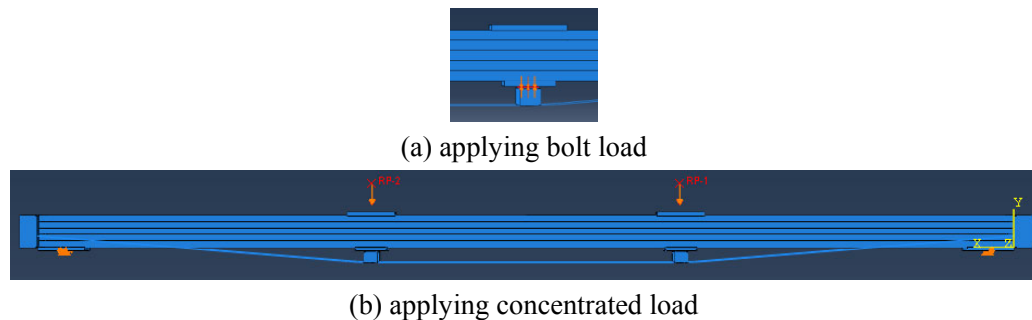


Figure 14: Simulated loading diagram

5.2 Feasibility verification

To verify the feasibility of the established model, simulated calculation is carried on the experiment. The load-deflection curve obtained from the experiment and the finite element analysis under the same working condition is compared, as shown in Fig. 15.

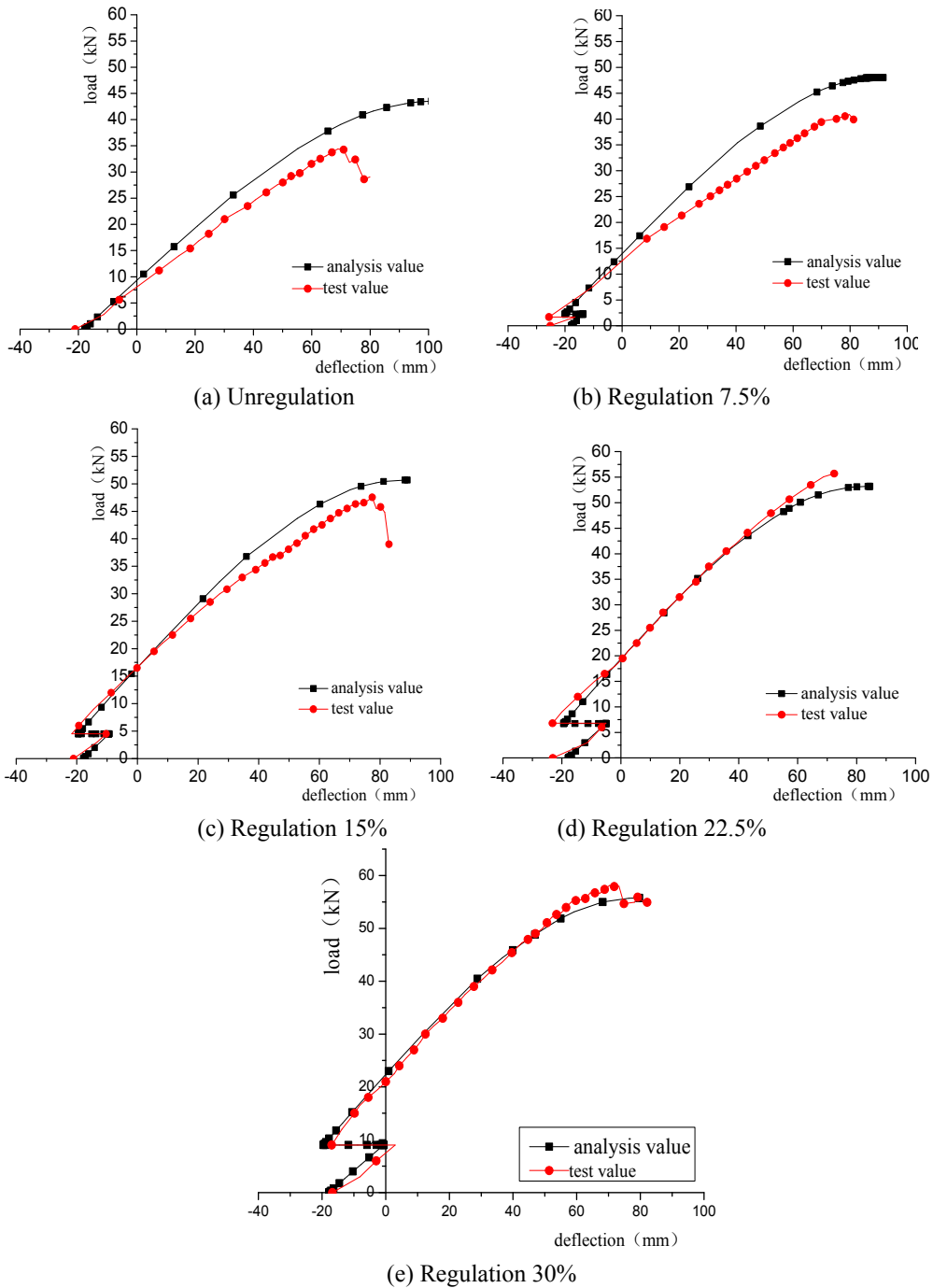


Figure 15: Comparison of load-deflection curve between model beam and experiment beam

As can be seen from Figs. 15(a)-15(b), the slope and the ultimate load of the load-deflection curve of the unregulated group and the regulated group of 7.5% are both larger than the experimental value, and the experiments of the regulated group of 15%, 22.5% and 30% are consistent with the load-deflection curve obtained by finite element analysis. The percentage difference of the ultimate load is 30.55%, 14.82%, 0.72%, 0.08% and 1.25% respectively. As a kind of natural material, wood has large dispersion. For the unregulated beam, the pre-stress applied in the experiment is relatively small, and the gap between anchors is large. The finite element analysis is in the ideal state, which makes the error between the experiment and the finite element analysis be 30.55%, which is relatively large. Based on the above analysis, the finite element model established in this section has small error and is consistent with the trend, so it can be used in the subsequent analysis.

5.3 Analysis of working condition

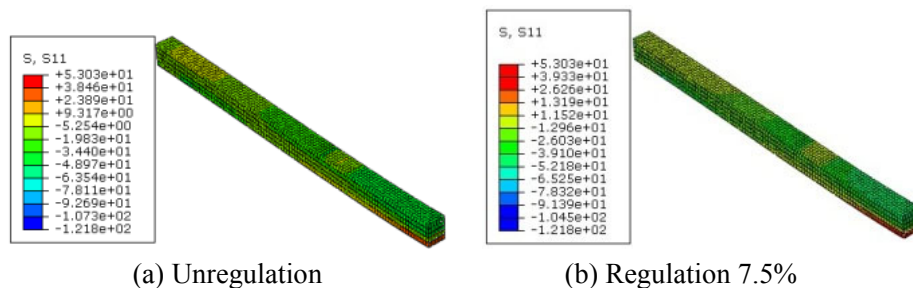
In order to find out the boundary of pre-stress regulation and control and give a reasonable regulation and control range, YTA6 and YTA7 are added in the finite element analysis compared with experiment group, totaling 7 working conditions, as shown in Tab. 4.

Table 4: Grouping of model beam

Beam number	Prestressing value/kN	Tendons No.	Degree of regulation
YA1	9	2	-
YTA2	9	2	7.5% of ultimate load
YTA3	9	2	15% of ultimate load
YTA4	9	2	22.5% of ultimate load
YTA5	9	2	30% of ultimate load
YTA6	9	2	37.5% of ultimate load
YTA7	9	2	45% of ultimate load

(2) Section stress distribution

To discuss the influence of the regulation and control amplitude on the stress distribution of the beam section, the stress nephogram of glulam beam at the time of failure is sorted and analysed, as shown in Fig. 16.



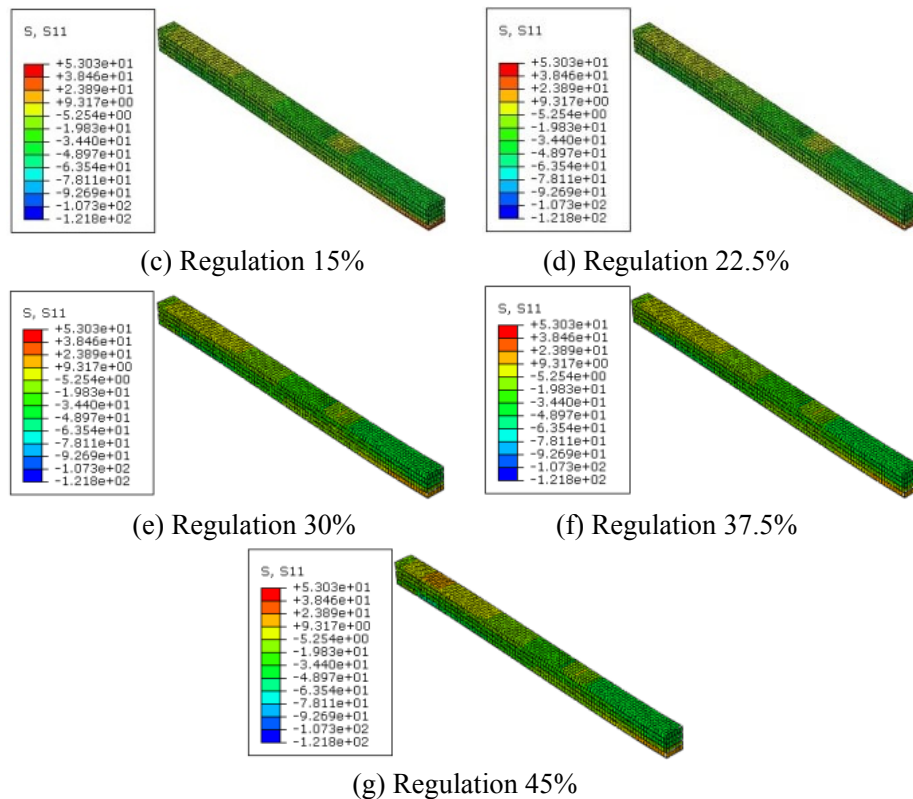


Figure 16: Stress nephogram of glulam at the time of failure of each model beam

It can be seen from Fig. 16 that the tension stress of the upper surface near the support tends to increase with the increase of regulation and control amplitude at the time of failure. The bottom tension stress of mid-span beam tends to decrease. At the time of failure, the glulam is subjected to two forces: the end concentrated force and the vertical concentrated force of the downwards two or three points of division, as shown in Fig. 17. The two forces produce a bending moment distribution of large mid-span and small ends, as shown in Fig. 18. With the increase of the regulation and control amplitude, the ultimate load increases and the tension stress of the steel wire increases, reducing the tension stress of the bottom of the beam. The greater the end concentrated force is, the greater the uniform bending moment at the end is. Therefore, the stress nephogram distribution at the time of failure is presented in the glulam beam.

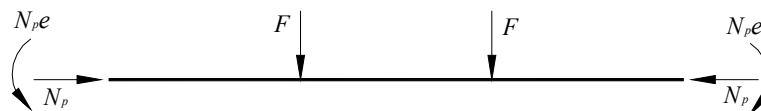


Figure 17: Equivalent load diagram of glulam beam section at the time of failure

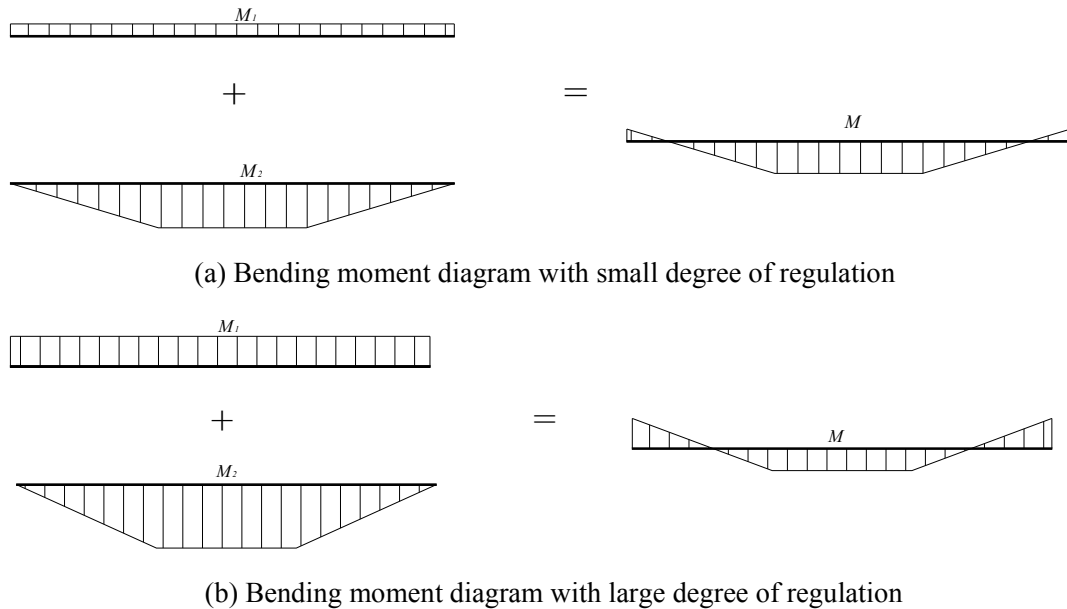


Figure 18: Bending moment diagram of glulam beam section at the time of failure

(3) Bearing capacity after regulation and control

After analysis, the bearing capacity of beam under different working conditions is summarized as shown in Tab. 5.

Table 5: Bearing capacity of beam under different working conditions

Beam number	Degree of regulation	Bearing capacity /kN
YA1	—	43.55
YTA2	7.5% of ultimate load	48.04
YTA3	15% of ultimate load	50.70
YTA4	22.5% of ultimate load	53.21
YTA5	30% of ultimate load	55.76
YTA6	37.5% of ultimate load	58.34
YTA7	45% of ultimate load	61.00

It can be seen from Tab. 5 that with the increase of regulation and control amplitude, the bearing capacity of pre-stressed glulam beam obtained by finite element analysis increases in turn. The bearing capacity of the regulated beam of 7.5%-45% increases by 10.31%-40.07% compared with the unregulated beam. The effect of regulation and control is obvious. The change trend of the ultimate load with the increase of the regulation and control amplitude is shown in Fig. 19. As can be seen from Fig. 19, the ultimate load of each beam basically increases linearly with the increase of the regulation and control amplitude.

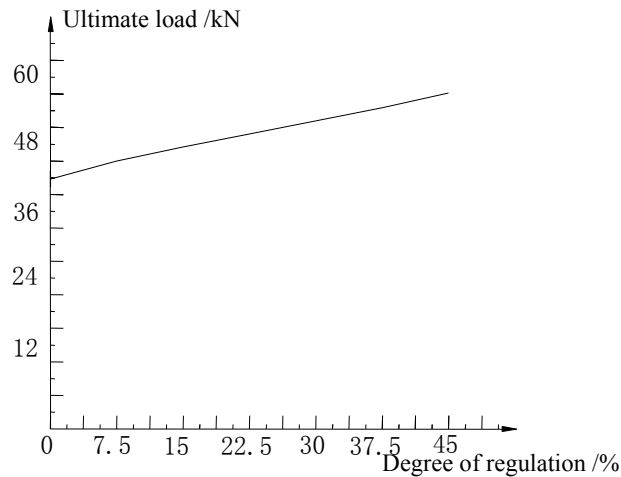


Figure 19: Change trend of the ultimate load

6 Long-term experiment

6.1 Experimental grouping

The glulam beam used in the long-term experiment is the same as that used in the short-term in design, processing and preliminary preparation, which will be give no more detailed description. According to the purpose of the experiment, five glulam string beams, which are the same as those used in the short-term bending experiment are produced and grouped into B groups. According to the initial load, they are divided into five types of working conditions. There is one beam in each working condition, including one unregulated beam, glulam string beams with regulation degree o of 7.5%, 15%, 22.5% and 30% of the ultimate load in the short-term experiment. According to the theoretical derivation of the project team in the early stage, 30% of the ultimate load in the short-term experiment is taken as the service load of beams in the long-term bending experiment [Yang (2015)]. The detailed grouping of the glulam string beams and the initial load and service load of different groups of beams in the long-term bending experiment are shown in Tab. 6.

Table 6: Preloading and service load of beams in the long-term bending experiment

Groups	Beam number	Average short-time ultimate load/kN	Initial load/kN	Service load/kN
Unregulation	YB1	33.36	-	10.01
Regulation 7.5%	YTB2	41.84	3.14	12.55
Regulation 15%	YTB3	50.34	7.55	15.10
Regulation 22.5%	YTB4	53.17	11.96	15.95
Regulation 30%	YTB5	55.07	16.52	16.52

Note: In the beam number YTBx in the table: letter Y represents the application of prestress; letter T represents the prestressing regulation; letter B represents the glulam

string beam group in the long-term bending experiment; and the Arabic numeral x represents the working condition number.

6.2 Process flow

In order to study the problem of stress reduction and increase in beam deflection in the prestressed tendon caused by the creeping of glulam in the long-term experiment under the regulation of different prestress, it is necessary to determine the influence of prestress regulation on the long-term bending performance of beams. The long-term experiment procedure is determined as follows: 1. Prepare the weight and weigh it, as is shown in Fig. 20. 2. Place all the experiment beams on the long-term loading experiment stand and connect the displacement meter, the glulam and steel strain gauges to the JM3813 multi-function static strain experiment system to prepare for the loading, as is shown in Fig. 21. 3. Apply a 9 kN prestress to the beam to obtain its inverse arch value. The process of applying prestress is the same as the short-term experiment and will not be described here. After the prestressing is applied, the inverse arch value f_1' at this time is recorded. 4. Apply different degree of initial load to force certain deflection of the beam. According to the situation of the short-term experiment, the initial load is not applied to unregulated beams and the initial load applied to the regulated beam is 7.5%, 15%, 22.5% and 30% of the ultimate load in the short-term experiment, namely 0, 3.14, 7.55, 11.96, 16.52 kN. First, two experimenters use the jack to lift the weight from both ends until the weight is off the ground, as is shown in Fig. 22; then, the weight is suspended with a steel wire rope at the point of bisection and trisection, and the duckbill is used to fix the joint of wire rope to prevent the slippage of steel wire rope caused by the heavy weight from, as is shown in Fig. 23; finally, the two experimenters simultaneously leak the jack and the weight is completely born by the glulam beam, which finishes the application of the initial load. At this time, the downward deflection f_2' produced by the beam is recorded. 5. Adjust the deflection of the beam to that before the application of the initial load by the prestressing device, which is to adjust the deflection of the beam to the inverse arch of the beam after the application of prestress. 6. Apply the service load maintain for 225 days. Gently place the prepared weight for the service load on the weight used for the initial load to complete the application of service load. The beam in the long-term loading is shown in Fig. 24.



Figure 20: Weigh weighing

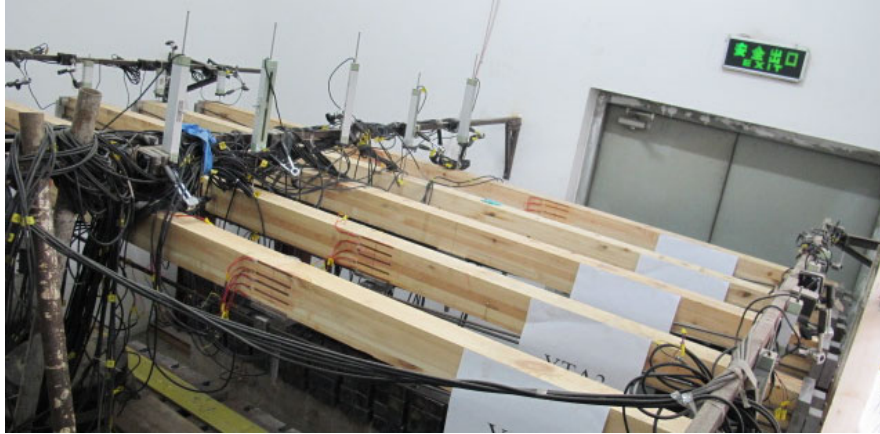


Figure 21: Preparing the experimental beam for loading



Figure 22: Lifting the weight with a jack



Figure 23: Using duckbill to fix the joint of steel rope



(a) Top view (b) Bottom view

Figure 24: Beams in long-term loading

6.3 Experiment phenomenon

For subsequent analysis, from the beginning to the end of the experiment, the glulam beam is observed and photographed at intervals, and the phenomenon during the creep is recorded. The state diagram of glulam beams at different times in the long-term experiment is shown in Fig. 25 to Fig. 29.



(a) Day 1 of the experiment

(b) Day 75 of the experiment



(c) Day 150 of the experiment

(d) Day 225 of the experiment

Figure 25: State diagram of long-term experiment YB1

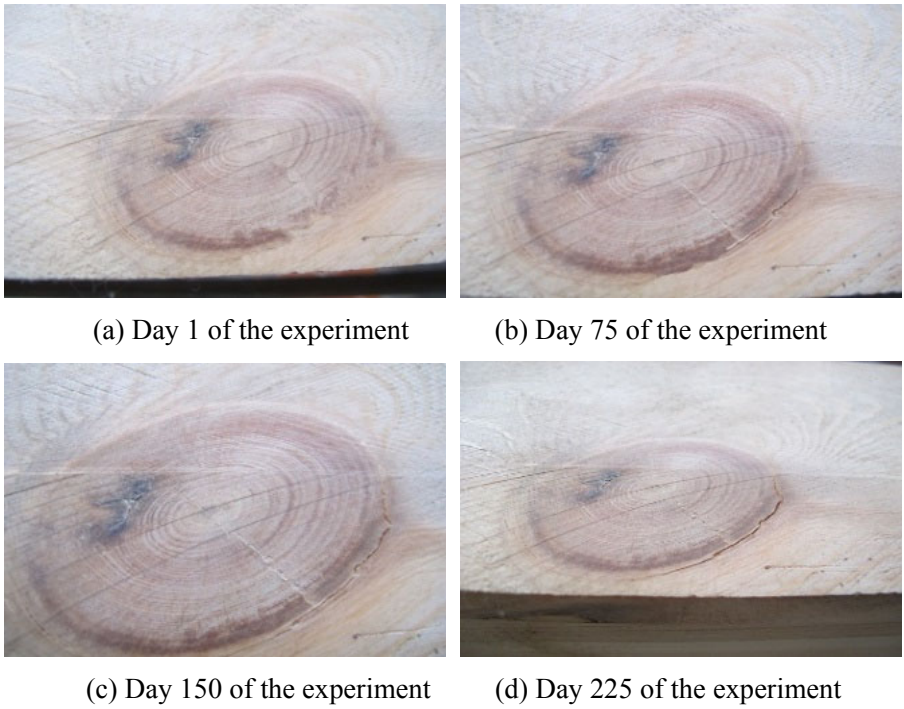


Figure 26: State diagram of long-term experiment YB2

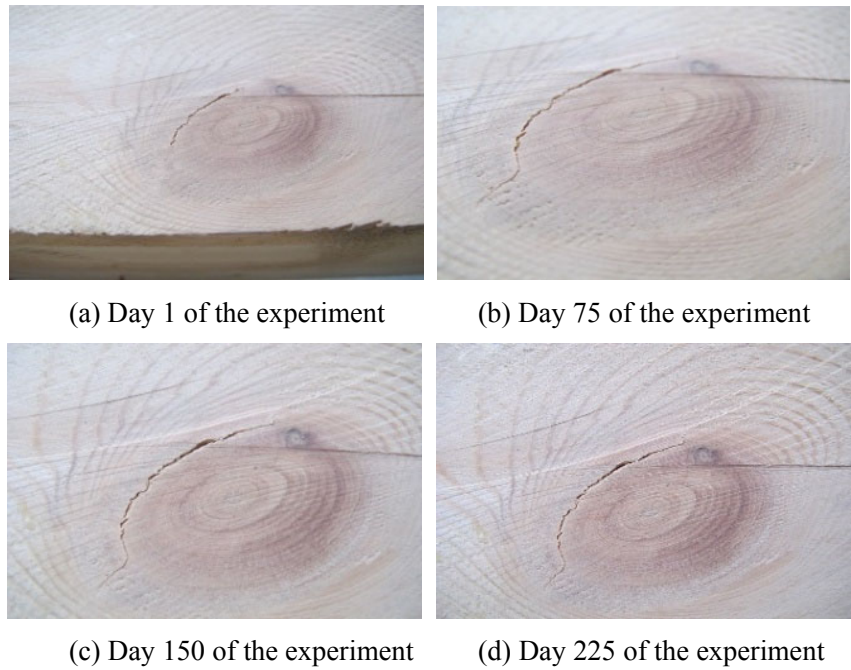


Figure 27: State diagram of long-term experiment YB3

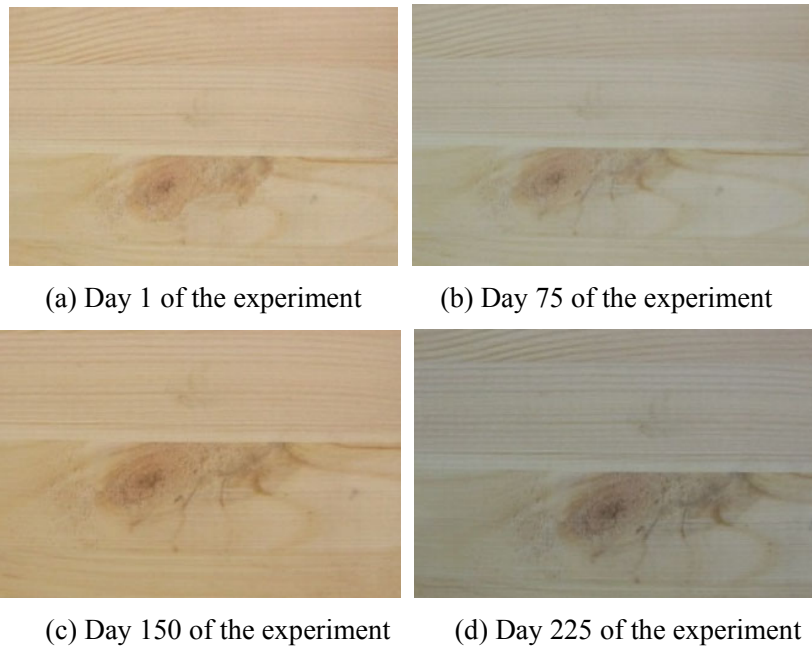


Figure 28: State diagram of long-term experiment YB4

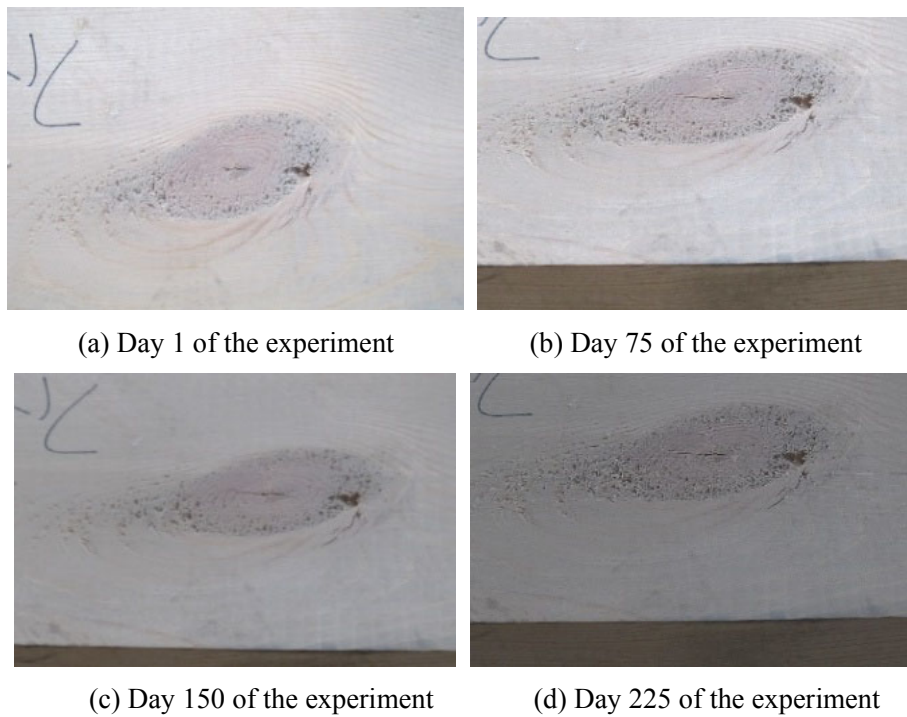


Figure 29: State diagram of long-term experiment YB5

It can be seen from Fig. 25 to Fig. 29 that compared with the first day of the experiment, the beam YB1 to YTB5 shows cracks slightly extending around the beam at the beam body at the 75th day of the experiment, and the crack on the 150th and 225th day at the late period later do not extend obviously. Since the applied load is the service load, which is only 30% of the ultimate load in the short-term experiment, the glulam beam is basically stable during the entire loading in the long-term experiment.

6.4 Experiment results and analysis

(1) Research on the law of stress variation of prestressed wire

The time-varying average stress of the four steel bars of the prestressed wire in the prestressed glulam string beam in the whole process from the initial loading to the end of loading is shown in Fig. 30.

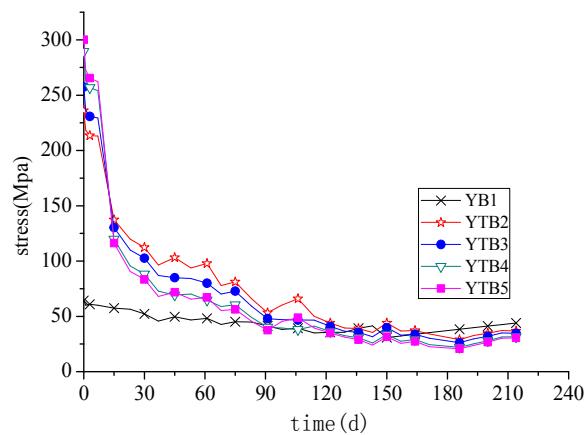


Figure 30: Time-varying curve of average stress of prestressed wire

It is known from Fig. 30 that the initial average stress of the beam YB1 to the beam YTB5 is 64.27, 235.97, 257.36, 289.45, and 300.14 Mpa respectively in the beginning and the average stress value of the steel wire decreases by 31.41%, 84.42%, 86.51%, 89.08% and 89.81% from the first day of the experiment to the 225th day of the experiment. It can be seen that with the increasing degree of prestressing regulation and the total pre-applied force, the initial average stress of the prestressed steel wire also increases, which leads to greater loss of the average stress of the steel wire; this is because the greater the regulation degree, the greater the bearing of the beam, which thus leads to greater applied service load. In terms of the analysis of the cross-section stress of the glulam, the greater the stress, the greater the creeping of the glulam. Thus, the stress loss of the steel wire is more significant. Secondly, on the 15th day of the experiment, the stress of the beam of 7.5%, 15%, 22.5% and 30% is degraded by 49.41%, 57.06%, 65.82%, and 68.23%, respectively. With the time going by, it gradually eases in the late stage. The reason for this phenomenon is may be fact that in the early stage of the experiment, there is a period of rapid development of the creeping in glulam, which leads to the fact that the stress degradation of steel wire reaches up to 50% at the initial stage.

In order to analyze the change rate of the average stress value of the steel wire in the beam, it is assumed that the initial average stress of the steel wire of each beam is zero. The variation of the average stress of the steel wire during the experiment is called the relative stress value and the time-varying curve of the relative stress of the prestressed steel wire is plotted, as is shown in Fig. 31.

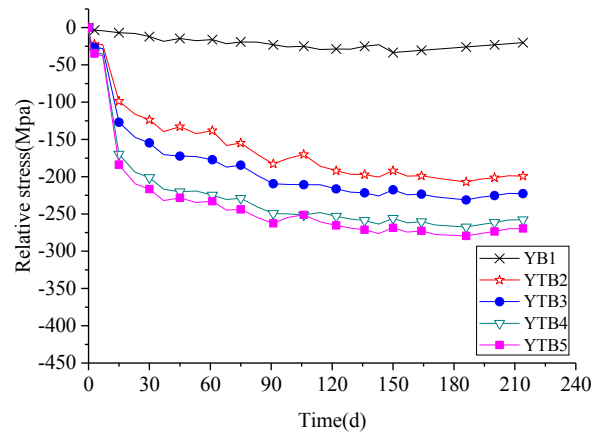


Figure 31: Time-varying curve of the relative stress of the prestressed steel wire

It can be seen from Fig. 31 that at the initial stage of loading, the greater the regulation degree, the faster the stress drop rate of the steel wire of the beam. However, with the passage of time, the drop rate of steel wire stress of all beams is basically the same in the later stage of the experiment. This shows that the effect of prestressing regulation on the drop rate of steel wire stress is more obvious in the early stage of the experiment. From the beginning to the end of the experiment, the variation of relative stress of the steel wire YTB2, YTB3, YTB4 and YTB5 is 9.87, 11.03, 12.77 and 13.35 times of the beam YB1 respectively, which indicates that the greater the regulation degree, namely the larger the total pre-applied force, the greater the variation of relative stress of the steel wire.

(2) Research on the change law of deflection in beam span

In the long-term loading experiment, the deflection change of the prestressed glulam beam includes the upward inverse arch when applying the prestressing force, the downward deflection caused by the application of the initial load, the upward inverse arch cause by the prestressing regulation, the instantaneous deflection cause by the application of service load and the creep deflection of the glulam after long-term creeping. In order to obtain the long-term deflection development rule of prestressed glulam string beams with different regulation degree, the time-deflection relationship curve is drawn as shown in Fig. 32. In the figure, the positive deflection indicates that the deflection is downward and the negative indicates that the deflection is upward.

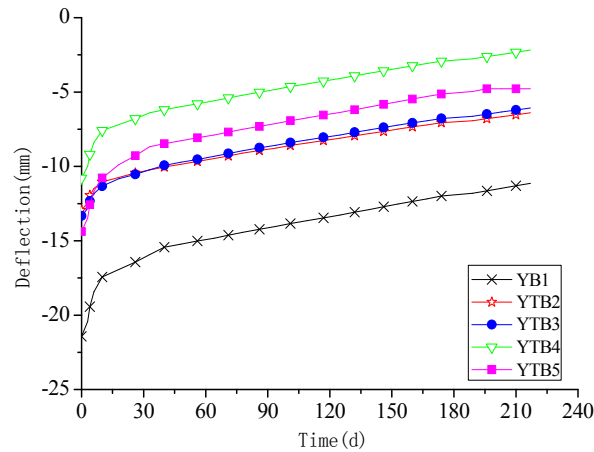


Figure 32: Time-varying curve of deflection in beam span

It can be seen from Fig. 32 that the deformation of the beam with the regulation of 7.5%, 30%, 34% and 45% of the total deformation at the 15th day of the experiment, which is also due to the existence of a rapid development period of creeping in the glulam during the beginning of the experiment; during the 225th day of the experiment, the deformation of the prestressed glulam beam increases by 10.52 mm, 6.20 mm, 7.25 mm, 8.61 mm and 10.07 mm, respectively, and the creep deformation of beam with the regulation of 7.5%, 15%, 22.5% and 30% is 58.94%, 68.92%, 81.84%, and 98.72% of unregulated beams. The reason is that the prestressing force applied to the unregulated beam is small and there is a gap between the anchors, so during the long-term loading, the gap will gradually close and the long-term deformation is large; the prestressing force applied by the regulated beam is large, the gap between the anchors is closed at the beginning of long-term loading, and the long-term deformation is small. The regulated beam has relative large prestressing force, so the gap between the anchors is closed in the early period of loading and the long-term deformation is larger. The greater the regulation degree, the greater the impact of creeping and the greater the long-term deformation.

In order to see the impact of the degree of prestressing regulation on the long-term creep rate of the beam more intuitively, the time-varying curve of the creep deformation in the prestressing glulam beam with different regulation degree is plotted, as is shown in Fig. 33.

It can be seen from Fig. 33 that from the 7.5%, 15% and 22.5% of the regulated and unregulated beam to the 30% of regulated beam, the creep rate in each beam span is relatively close from the beginning to the end of the experiment. This is because with the increase of the regulation degree, the creep of the beam becomes larger. However, at the same time, the regulation also increases the internal force arm of the beam so that the creep rate of each beam span is relatively close to one another.

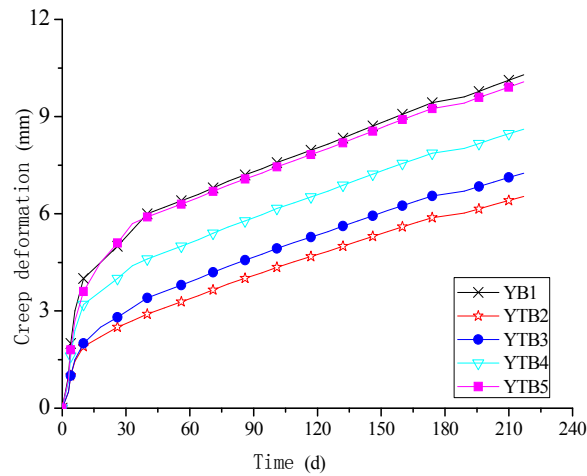


Figure 33: Time-varying curve of the creep deformation in the prestressing glulam beam

6.5 Establishment and prediction of creep model

(1) Selection of creep model

The characteristic that wood deformation increases with time under a constant load is called the creep of wood. The additional deformation effect caused by the creep of the wood can increase the overall deformation of the prestressed glulam string beam and even affects its normal use, thus reducing its durability. It is a straightforward and effective way to establish the creep model of wood to fit the experiment data to calculate and predict the additional deformation caused by the creep of wood. Referring to the previous research results, this paper uses the power-law model for the fitting of experimental data and the prediction of deformation of the creep of five beams in the long-term experiment. The time-varying formula of mid-span deflection can be derived from the power-law model:

$$y = At^B + C \quad (8)$$

In the formula:

y -the mid-span deflection value of the glulam beam (mm);

t -the time of creep deformation of the glulam beam (t);

A, B, C-experiment parameters, derived from the fitted curve.

Through the custom function of origin software, the power-law model formula is used for the fitting analysis of the creep data of five beams in the long-term experiment. The creep fitting curve of each beam is shown in Fig. 34.

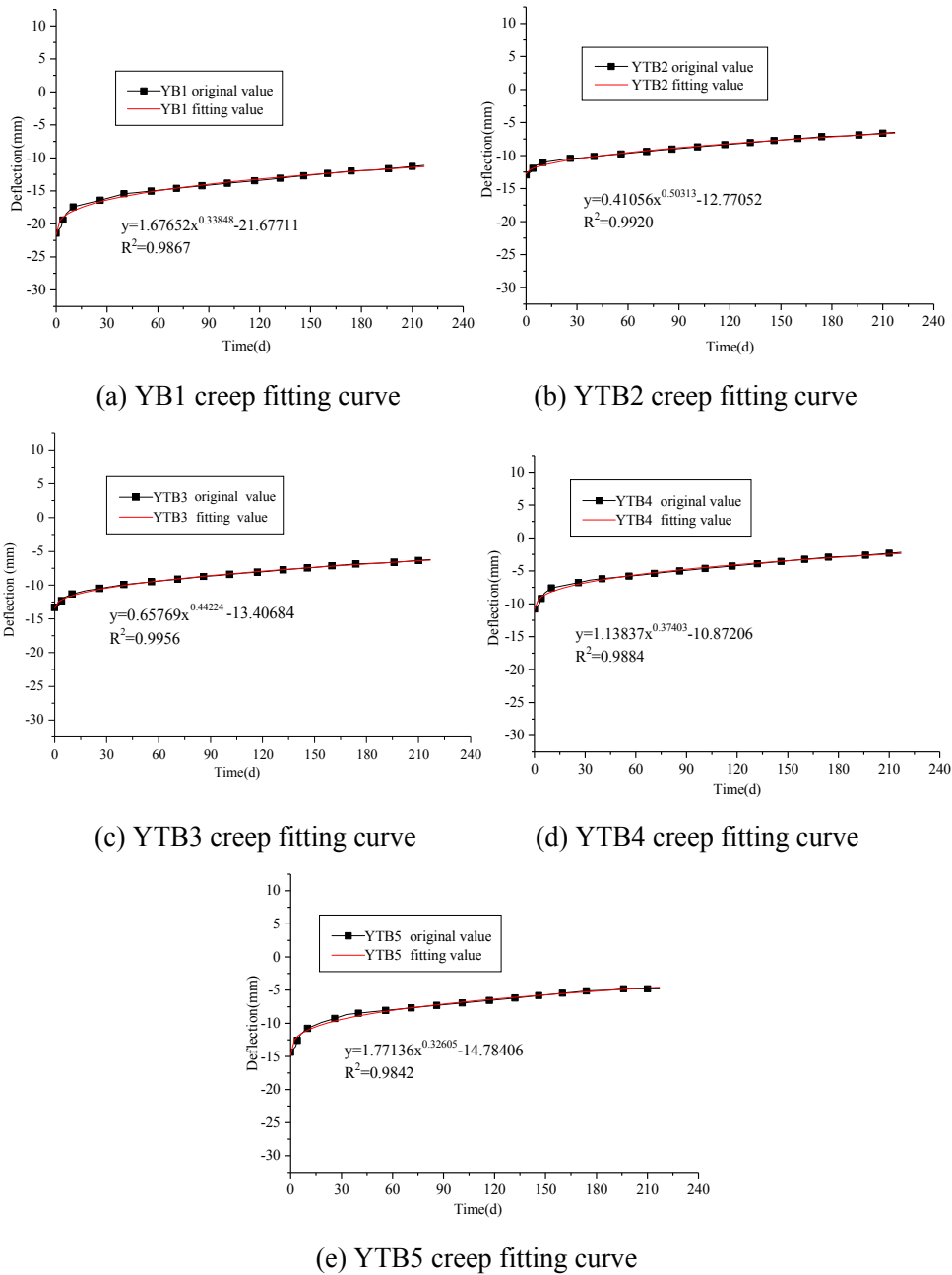


Figure 34: Creep fitting curve of each beam

The experiment parameter A, B, C and correlation coefficient R2 of the fitting curve of each beam are shown in Tab. 7.

Table 7: Result of fitting parameters

Beam number	A	B	C	R2
YB1	1.67652	0.33848	-21.67711	0.9867
YTB2	0.41056	0.50313	-12.77052	0.9920
YTB3	0.65769	0.44224	-13.40684	0.9956
YTB4	1.13837	0.37403	-10.87206	0.9884
YTB5	1.77136	0.32605	-14.78406	0.9842

It can be seen from Tab. 7 that the correlation coefficients of the five sets of fitting curves are greater than 0.98, indicating that the fitting accuracy between the result of experimental data in Fig. 34 and the result in fitting formula is high, which can well reflect the long-term creep characteristics of glulam.

(2) Rationality verification of creep model

In order to verify the rationality of the creep model, the YTB3 beam is taken as an example. The creep deformation of the beam at 20, 40, ... 220d is calculated and predicted by the power-law model fitting formula, which is compared with the experimental value, as is shown in Tab. 8.

Table 8: Experiment value and predicted value of YTB3 mid-span deflection

Time (d)	Test value (mm)	Predictive value (mm)	Percentage error
20	-10.73	-10.93	1.94
40	-9.93	-10.05	1.21
60	-9.43	-9.39	0.42
80	-8.86	-8.84	0.17
100	-8.40	-8.37	0.35
120	-7.93	-7.94	0.22
140	-7.55	-7.56	0.16
160	-7.08	-7.20	1.79
180	-6.66	-6.87	3.22
200	-6.63	-6.56	1.01
220	-6.08	-6.26	3.09

It can be seen from the result in Tab. 8 that the error percentage of the experimental value and the predicted value is mostly less than 10%, indicating that the power-law model is more accurate for the calculation and prediction of creep deformation in the long-term experiment.

(3) Calculation of long-term deflection

Considering that the calculation method for long-term deformation is not given in China's "Code for Design of Wood Structures" (GB50005-2003), this paper draws on the European design code and a thesis [Chen (2017)]. Under the long-term loading, the

additional deflection value generated from the creep of the glulam beam will be converted into an increase factor, ie, a creep deformation coefficient, to calculate its long-term deflection. The creep deformation coefficient θ is defined as the ratio of the additional deflection generated by the creep of the glulam beam under long-term load to the elastic deflection generated under the load [Chen (2017)]. The creep deformation coefficient formula is as follows:

$$\theta = \frac{f_c}{f_s} = \frac{f_L - f_s}{f_s} \quad (9)$$

In this formula: θ -creep deformation coefficient;

f_c -the additional deflection value produced by the creep of the glulam beam;

f_L -the long-term deflection value of the glulam beam;

f_s - the elastic deflection value produced by the load.

Since the design life of general buildings is 50 years, this paper uses the power-law model formula to predict the long-term deflection value of the glulam beam for 50 years, and then calculates the creep deformation coefficient. The specific value of the creep deformation coefficient of each experimental beam is shown in Tab. 9.

Table 9: Creep deformation coefficient table

Beam number	Elastic deflection/mm	Long-term deflection of fifty years/mm	Coefficient of creep deformation θ
YB1	7.34	24.75	2.37
YTB2	16.04	44.42	1.77
YTB3	13.03	37.00	1.84
YTB4	10.21	33.81	2.31
YTB5	8.10	28.64	2.54

It can be seen from Tab. 9 that for the glulam beam with different regulation degree, the creep deformation coefficient increases with the regulation degree. This is because the greater the regulation degree, the greater the prestress applied to the beam, and the greater the bearing of the beam, the corresponding long-term load value will also increase so that the creep deformation of wood will increase with the regulation degree, which thus increase the creep deformation coefficient of the prestressed glulam beam.

According to the research content in this paper, Tab. 9 and the above analysis results, it is suggested that the creep deformation coefficient can be 1.77 to 2.54 for the theoretical calculation of the prestressed glulam beam.

7 Conclusions

(1) The failure mode and ultimate load of all beams under 5 short-term working conditions are analyzed through flexural experiment. The compression failure amounts to 90% of the total failure amount, showing that regulation and control can obviously improve the failure mode of string beam of glulam and make full use of the compressive

property of wood. The ultimate load of the regulated beam is obviously larger than that of the unregulated beam, and the ultimate load of the beam increases with the increase of the regulation and control amplitude. Compared with the unregulated beam, the ultimate load of the regulated beam of 7.5%-30% increases by 25.42%-65.08%, and the regulation and control effect is obvious.

(2) By drawing the load-deflection curve, it is found that the slope and the peak value increase with the increase of the pre-stress regulation and control amplitude, that's, the stiffness and the bearing capacity of the beam increase.

(3) By drawing the load-strain curve, it is found that there are 3 layers of glued plates in compression zone when the beams in unregulated group and regulated groups of 7.5% and 15% are damaged and there are 4 layers of glued plates in compression zone when the beams in unregulated group and regulated groups of 22.5% and 30% are damaged. This shows that the compression height of beam increases before the failure with the increase of the regulation and control amplitude, and it reaches the state of full section compression at the time of failure, fully exerting the compressive strength of the glulam.

(4) Based on the short-term force analysis of typical failure mode of glulam beam, the bearing capacity calculation formulas of string beam of pre-stressed glulam under three kinds of failure modes: tension crack on the top, un-tension crack on the top and compression failure at the bottom of glulam beams are derived.

(5) Based on the finite element analysis of the beam under 7 working conditions, it is found that the tension stress of the upper surface near the support tends to increase with the increase of the regulation and control amplitude at the time of failure. The bottom tension stress of mid-span beam tends to decrease. In addition, with the increase of regulation and control amplitude, the bearing capacity of the pre-stressed glulam beam obtained by finite element analysis increases in turn. Compared with the unregulated beam, the bearing capacity of the beam regulated by 7.5%-45% increases by 10.31%-40.07%, and the regulation and control effect is obvious.

(6) After the short-term tests of the creep beams, the ultimate load increases with the increase of the control degree. Compared with the beam without regulation, the ultimate load of the beam with regulation of 7.5%, 15%, 22.5% and 30% increased by 4.90%, 14.21%, 22.73% and 37.16%, respectively. Compared with the uncreep beam, the ultimate load of the creep beam is greatly improved. By comparing the load-deflection curves of the creep and non-creep beams, it is found that the stiffness and bearing capacity of the creep beams have been greatly improved, and the ultimate deflection and ductility have not been greatly affected, which is almost the same with the non-creep beams. This indicates that the creep effect on the stiffness and bearing capacity of prestressed beams is obvious.

Acknowledgement: In the process, this project was supported by the Fundamental Research Funds for the Central Universities (2572017DB02), Natural Science Foundation of Heilongjiang Province (JJ2019LH0696), and by Postdoctoral Scientific Research Developmental Fund of Heilongjiang Province in 2016 (LBH-Q16011).

Reference

Anshari, B.; Guan, W. Z.; Kitamori, A.; Jung, K.; Komatsu, K. (2012): Structural behaviour of glued laminated timber beams pre-stressed by compressed wood. *Construction and Building Materials*, vol. 29, pp. 24-32.

Chen, H. (2017). *The Study on Flexural Performance of Regulable Reinforcement Glulam Beams Based on the Creep Behavior (Ph.D. Thesis)*. Northeast Forestry University, China.

D'Aveni, A.; D'Agata, G. (2017): Post-tensioned timber structures: new perspectives. *Construction and Building Materials*, vol. 153, pp. 216-224.

Fang, H.; Sun, H.; Liu, W.; Wang, L.; Bai, Y. et al. (2015): Mechanical performance of innovative GFRP-bamboo-wood sandwich beam experimental and modelling investigation. *Composites Part B: Engineering*, vol. 79, pp. 182-196.

Fava, G.; Carvelli, V.; Poggi, C. (2013): Pull-out strength of glued-in FRP plates bonded in glulam. *Construction and Building Materials*, vol. 43, no. 2, pp. 362-371.

Ferrier, E.; Labossière, P.; Neale, K. W. (2012): Modelling the bending behaviour of a new hybrid glulam beam reinforced with FRP and ultra-high-performance concrete. *Applied Mathematical Modelling*, vol. 36, no. 8, pp. 3883-3902.

Franke, S.; Franke, B.; Harte, M. A. (2015): Failure modes and reinforcement techniques for timber beams-state of the art. *Construction and Building Materials*, vol. 97, pp. 2-13.

Green, W. D.; Winandy, E. J.; Kretschmann, E. D. (1999): *Wood Handbook Chapter 4: Mechanical Properties of Wood*. Forest Products Laboratory, Wisconsin.

Guan, W. Z.; Rodd, D. P.; Pope, J. D. (2005): Study of glulam beams pre-stressed with pultruded GRP. *Computers & Structures*, vol. 83, no. 28-30, pp. 2476-2487.

Guo, N.; Chen, H.; Zhang, P.; Zuo, H. (2016): The research of parallel to the grain compression performance test of laminated glued bamboo-wood composites. *Technical Gazette*, vol. 23, no. 1, pp. 129-135.

Guo, N.; He, T.; Chen, H. (2015): The research of the influence of constitutive relation on glued- timber beam bending performance analysis results. *International Journal of Earth Sciences and Engineering*, vol. 8, pp. 665-670.

Guo, N.; Jiang, H.; Zuo, H. (2017): The research on flexural behavior experiment of prestressed glue-lumber beams after long-term loading. *Modelling, Measurement and Control B*, vol. 86, no. 1, pp. 49-62.

Guo, N.; Wang, Y.; Zuo, H. (2017): Study of short-term flexural behavior for glue-bamboo and lumber beams under different pre-stressed states. *The Civil Engineering Journal*, vol. 12, pp. 128-142.

Issa, A. C.; Kmeid, Z. (2005): Advanced wood engineering: glulam beams. *Construction and Building Materials*, vol. 19, no. 2, pp. 99-106.

Luca, D. V.; Marano, C. (2012): Prestressed glulam timbers reinforced with steel bars. *Construction and Building Materials*, vol. 30, no. 5, pp. 206-217.

- McConnell, E.; McPolin, D.; Taylor, S.** (2014): Post-tensioning of glulam timber with steel tendons. *Construction and Building Materials*, vol. 73, pp. 426-433.
- Negrão, H. J.** (2016): Preliminary study on wire prestressing methods for timber pieces reinforcement. *Construction and Building Materials*, vol. 102, pp. 1093-1100.
- Ribeiro, S. A.; Abílio, M. P. de Jesus; Lima, M. A.; Lousada, C. L.** (2009): Study of strengthening solutions for glued-laminated wood beams of maritime pine wood. *Construction and Building Materials*, vol. 23, no. 8, pp. 2738-2745.
- Sinha, A.; Way, D.; Mlasko, S.** (2014): Structural performance of glued laminated bamboo beams. *Journal of Structural Engineering*. vol. 140, no. 1, pp. 1-8.
- Toratti, T.; Schnabl, S.; Turk, G.** (2014): Reliability analysis of a glulam beam. *Structural Safety*, vol. 29, no. 4, pp. 279-293.
- Uzel, M.; Togay, A.; Anil, Ö.; Söğütü, C.** (2017): Experimental investigation of flexural behavior of glulam beams reinforced with different bonding surface materials. *Construction and Building Materials*, vol. 158, pp. 149-163.
- Wei, Y.; Ji, X.; Duan, M.; Li, G.** (2017): Flexural performance of bamboo scrimber beams strengthened with fiber-reinforced polymer. *Construction and Building Materials*, vol. 142, pp. 66-82.
- Yahyaei-Moayyed, M.; Taheri, F.** (2011): Creep response of glued-laminated beam reinforced with pre-stressed sub-laminated composite. *Construction and Building Materials*, vol. 25, no. 5, pp. 2495-2505.
- Yahyaei-Moayyed, M.; Taheri, F.** (2011): Experimental and computational investigations into creep response of AFRP reinforced timber beams. *Composite Structures*, vol. 93, no. 2, pp. 616-628.
- Yang, H.; Ju, D.; Liu, W.; Lu, W.** (2016): Prestressed glulam beams reinforced with CFRP bars. *Construction and Building Materials*, vol. 109, pp. 73-83.
- Yang, H.; Liu, W.; Lu, W.; Zhu, S.; Geng, Q.** (2016): Flexural behavior of FRP and steel reinforced glulam beams: experimental and theoretical evaluation. *Construction and Building Materials*, vol. 106, pp. 550-563.
- Yang, Y.** (2015). *The Study on Flexural Performance of Prestressed Glulam Beam String Structure Based on the Creep Behavior (Ph.D. Thesis)*. Northeast Forestry University, China.
- Zhao, T.** (2015). *Study of Short-Time Flexural Behavior for Glulam String Beams in Different Prestressed State (Ph.D. Thesis)*. Northeast Forestry University, China.
- Zhong, Y.; Wu, G.; Ren, H.; Jiang, Z.** (2017): Bending properties evaluation of newly designed reinforced bamboo scrimber composite beams. *Construction and Building Materials*, vol. 143, pp. 61-70.